Sectorization with Beam Pattern Design Using 3D Beamforming Techniques

Chang-Shen Lee, Ming-Chun Lee, Chung-Jung Huang, and Ta-Sung Lee
Department of Electrical Engineering, National Chiao Tung University, Taiwan, ROC
E-mail: {ben3003neb.cm01g@, leemingchun.cm01g@, chesterhuang.cm96g@g2., tslee@mail.}nctu.edu.tw
Tel: +886-3-5712121

***Abstract*— This paper presents a framework for a three-dimensional (3D) beam pattern design with a load-balanced cell sectorization strategy. First, characteristics of the 3D beam pattern were observed, and convex optimization was used to provide a solution based on the criteria that describe the observations. In addition, a user equipment (UE) determination problem that arose because of cell sectorization was also addressed. By incorporating a beam pattern design with a proposed UE determination scheme, a framework of a backward compatible system was completed. The network performance regarding throughput for cell sectorization with a dedicated beam pattern design was evaluated and the simulation results show that the proposed system is superior compared to the conventional system and other proposed sectorization schemes.**

Index Terms:— 3D beamforming, beam pattern design, cell sectorization, massive MIMO

I. INTRODUCTION

A downlink throughput can be potentially increased by providing degrees of freedom (DOF) on spatial domain. Multiuser (MU) multiple-input multiple-output (MIMO) techniques can provide the DOF using multiple antennas, which increase the throughput compared to a single antenna transmission. In 3rd Generation Partnership Project (3GPP) long-term evolution-advanced (LTE-A), evolved NodeB (eNodeB) has been equipped with multiple antennas to increase the throughput. In long-term evolution (LTE) Release 12, the 3GPP tries to utilize the vertical degrees of freedom. Therefore, a massive MIMO, which involves equipping more than one hundred antenna elements using independent weight at eNodeB becomes a potential solution to further increase the throughput. However, treating each antenna as an independent antenna port entails increasing the overhead of the feedback of the channel state information (CSI). However, the size of the massive MIMO system makes feedback impossible. Alternatively, because of the mature development of three-dimensional (3D) beamforming techniques, grouping many elements into several antenna ports and using 3D beamforming in each antenna port enables the efficient use of spatial DOF with limited CSI feedback, making this a promising and feasible application of the massive MIMO techniques in LTE-A.

In earlier works, [1]-[3] have confirmed that vertical sectorization and horizontal sectorization can increase system throughput. A study on beam pattern design using convex optimization [4] shows that beam pattern with arbitrary main lobe shape and sidelobe level is achievable using a sufficient number of antennas through convex optimization under conditions of symmetry constraints. However, previous studies did not incorporate the beam pattern design method with sectorization; moreover, because the desired beam pattern is usually not symmetric in practice, system performance can be further improved when the symmetry constraint in [4] is removed. In addition, the traffic load is an important factor in practice; however, in [1] the traffic load is unbalanced among the sectors. Furthermore, previous studies did not notice the user equipment (UE) position determination problem because the eNodeB must know the sector in which each UE is located, which is necessary when UE tries to access the network.

In this paper, to efficiently use the spatial DOF, a load-balanced cell sectorization scheme and the corresponding beam pattern design using 3D beamforming techniques are proposed. Moreover, the UE position determination problem arising from cell sectorization is addressed, and a potential solution is proposed. Therefore, a framework for system design that is backward compatible with the current systems is given, and the performance improvement is shown in simulations.

The rest of paper is organized as follows: Section II describes the proposed system model. The sectorization and beam pattern design schemes and the corresponding UE position determination scheme are discussed in Section III. Simulation results are shown in Section IV. Conclusions are discussed in Section V.

II. GENERAL INSTRUCTIONS

A rectangular planar array is composed of M and N identical antenna elements in y and z directions, respectively. The corresponding inter-element spacing is denoted as d_y and d_z in y and z directions. By defining $u_y=\sin\theta\sin\phi$ and $u_z=\cos\theta$, the beam pattern can be expressed as

$$G(u_y,u_z)=\sum_{m=1}^{M}\sum_{n=1}^{N}A(\theta,\phi)w_{m,n}^{*}e^{j\frac{2\pi}{\lambda}md_yu_y+j\frac{2\pi}{\lambda}nd_zu_z}, \quad (1)$$

where ϕ and θ are the azimuth and elevation angles in spherical coordinates, respectively. In addition, $G(u_y,u_z)$ can be represented as a vector product $A(\theta,\phi)\mathbf{w}^H\mathbf{s}$, where $\mathbf{w}\in\mathbb{C}^{MN}$ is composed of $w_{m,n}$ for $n=1,...,N$ and $m=1,...,M$, and $\mathbf{s}\in\mathbb{C}^{MN}$ is the corresponding steering vector.

This work was in part funded by the Aiming for the Top University and Elite Research Center Development Plan, and the MediaTek research center at National Chiao Tung University.

According to [5], the azimuth and the elevation radiation pattern for a single element are defined as (2) and (3), respectively.

$$A(\phi) = -\min\left[12\left(\frac{\phi}{\phi_{3dB}}\right)^2, A_m\right], \; A_m = 25dB, \tag{2}$$

$$A(\theta) = -\min\left[12\left(\frac{\theta}{\theta_{3dB}}\right)^2, SLA_v\right], \; SLA_v = 20dB, \tag{3}$$

where the front-to-back attenuation and sidelobe attenuation are denoted as A_m and SLA_v, respectively. According to [5], the 3D synthesized beam pattern can be formulated as follows:

$$A(\phi,\theta) = -\min\left[-\min[A_H(\phi) + A_E(\theta)], A_m\right]. \tag{4}$$

To execute a performance evaluation, the signal-to-interference-plus-noise ratio (SINR) is measured at the ground level and is given by

$$SINR_{i,(\theta,\phi)} = \frac{P^M_{i,(\theta,\phi)}}{\sum_{j=1, j\neq i}^{N} P^L_{j,(\theta,\phi)} + \sigma_n^2}, \tag{5}$$

where $P^M_{i,(\theta,\phi)}$ is the power of the corresponding main beam for sector i and direction (θ,ϕ), $P^L_{i,(\theta,\phi)}$ is the leakage power from other sectors or cells, and σ_n^2 is the noise power.

III. Problem Formulation and Beam Pattern Design

In this section, a framework of cell sectorization strategy and corresponding beam pattern design is introduced. Subsequently, a proposed solution for the arising UE position determination problem after sectorization is proposed.

A. *Cell Sectorization and the Corresponding Beam Pattern Design*

The aim of the approach is to efficiently utilize both vertical and horizontal spatial DOFs. The adopted approach involves partitioning the cell into smaller sectors and using 3D beamforming techniques to form corresponding beams in each sector. In addition, the traffic load balance issue is emphasized as a critical factor that affects the efficiency of frequency reuse. Therefore, the cell should be partitioned according to the traffic load distribution. Based on this observation, the remaining task is to construct beam patterns that target the corresponding sectors without causing interference with other sectors and cells. Generally, the cell could be partitioned vertically or horizontally into arbitrary number of sectors, but the feasibility of the corresponding beam patterns depend on the number of antennas used. If a cell is partitioned into too many sectors but the number of antennas is relatively small, the beam patterns satisfying all the constraints (main beam width, sidelobe level, etc) may be infeasible akin to the filter design. The detail relation between performance and number of sectors in a cell for a fixed antenna array is complicated and need further study. In this work, the 3 × 3 cell is proposed as a framework of higher order sectorization using 3D beamforming. The cells with different sectorization schemes are shown in Fig. 1. In the proposed 3 × 3 cell, all sectors have an equal area because the uniform distribution of user traffic is assumed. The boundary between sectors is defined by a pair of ranges of elevation angle (θ) and azimuth angle (ϕ). The boundaries are listed as follows:

$$\begin{aligned} &\text{Sector 1:} \; 102^\circ < \theta < 180^\circ, \quad -60^\circ < \phi < 60^\circ \\ &\text{Sector 2:} \; 97.3^\circ < \theta < 102^\circ, \quad -60^\circ < \phi < 0^\circ \\ &\text{Sector 3:} \; 97.3^\circ < \theta < 102^\circ, \quad 0^\circ < \phi < 60^\circ, \end{aligned} \tag{6}$$

To make an appropriate beam pattern, several key points must be noticed. First, nulls always exist when beamforming is used. The spatial response $\mathbf{w}^H\mathbf{s}(\theta,\phi)$ was set to one for the desired area to prevent the desired sector from a low signal power problem caused by nulls toward the desired sector.

Second, because the formation of sidelobes is inevitable when using beamforming. For other sectors or cells in which the same frequency band is used as a desired sector, the corresponding spatial response $\mathbf{w}^H\mathbf{s}(\theta,\phi)$ should be less than l_i to minimize the interference to those sectors or cells. Conversely, for sidelobes that face the sky or other sectors or cells in which using a different frequency band does not cause interference, the corresponding spatial response $\mathbf{w}^H\mathbf{s}(\theta,\phi)$ should be less than l_j to minimize wasting transmission power. The constraints for sidelobes causing power waste are looser than those causing interference in this study. However, these constraints are necessary otherwise most of the transmit power would target the sky or other undesired area causing severely degradation of the performance. Therefore, to efficiently use the limited DOF, which is proportional to the number of antennas used, l_i for sidelobes causing interference is set smaller than l_j for sidelobes causing power waste.

For weight vectors $\mathbf{w}$ that satisfy the aforementioned constraints, the vector with the minimal norm $\|\mathbf{w}\|$ is preferred, because it represents the vector with minimal transmission power. The mentioned constraints can be formulated as a convex optimization problem as follows:

$$\begin{aligned} &\underset{\mathbf{w}}{\text{minimize}} && \|\mathbf{w}\| \\ &\text{subject to} && \mathbf{w}^H\mathbf{s}(\theta,\phi) = 1, \{\theta,\phi\} \in U_0 \\ &&& \mathbf{w}^H\mathbf{s}(\theta,\phi) \le l_i, \{\theta,\phi\} \in U_i, i = 1,2,\cdots,m \\ &&& \mathbf{w}^H\mathbf{s}(\theta,\phi) \le l_j, \{\theta,\phi\} \in U_j, j = 1,2,\cdots,n. \end{aligned} \tag{9}$$

The set U_0 the constraints on the main beam and U_i represent the constraints on the sidelobes. The problem above has similar form to the one in [4]; nevertheless, the optimal beam pattern is not symmetric in our problem, thus the symmetry constraint on the beam pattern in [4] must be

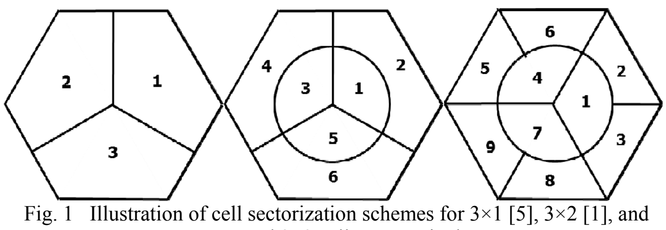

Fig. 1 Illustration of cell sectorization schemes for 3×1 [5], 3×2 [1], and proposed 3×3 cells, respectively.

removed, and the optimal weight vector becomes a complex vector. Thanks to the mature development of convex optimization tools [6], the optimal weight vector **w** can be obtained using a SeDuMi MATLAB toolbox. The beam patterns of proposed 3 × 3 cell are shown in Fig. 2 and Fig. 3.

Although the beam pattern is designed to meet the statistical traffic load based on geometry, having an equal load on each sector in practice is difficult. Because the optimal weight vector **w** does not guarantee that every point inside the target sector has high received power for a given beam, areas in which the signal power is relative low persist; thus users in those areas should be assigned to other beams because they can receive stronger power from them. By considering a traffic load and beam pattern design with practical observations and constraints, the proposed framework provides a fair SINR on every point inside the cell.

B. Proposed UE Position Determination Approach

After applying sectorization to existing LTE-A systems, a new problem arises: the eNodeB must know the sectors in which each user is located. To solve this problem, a simple but efficient and reliable solution is proposed by exploring the existing precoder matrix indicator (PMI) and channel quality indicator (CQI) feedback mechanism in LTE-A. This solution simply modifies eNodeB behavior without affecting UE, and is backward compatible and can be applied to current systems.

In the LTE-A systems, the overall downlink bandwidth is divided into several sub-bands with equal size. UE reports its own CQI aperiodically on each sub-band according to the quality of the corresponding received pilot signal [7]. Therefore, the power disparity of the downlink reference signal on each sub-band can be intentionally designed in eNodeB end (e.g. UEs in different sector receive different power levels of the downlink reference signal in each sub-band). Because of the power disparity, the CQI report is correlated to the power disparity produced by the eNodeB. Thus, from the CQI report, the eNodeB locate the UE. For example, the power levels of reference signals for sector 1, 2, and 3 can be $[P_1, P, P, P]$, $[P, P_2, P, P]$, $[P, P, P_3, P]$, respectively, where P_1, P_2, P_3 should be significantly different from P. If the location of the user is Sector 2, the CQI report of this user suggests that the CQI of sub-band 2 is considerably different compared with the other sub-bands. Thus, the eNodeB can determine the location of each user.

The concept of this solution is similar to pulse amplitude modulation (PAM) because information is contained in the power level. Through this solution, the position of UE can be determined without additional UE feedback information or updating the UE device; therefore, the proposed solution is potentially backward compatible for the LTE-A UEs. In addition, the proposed solution determines the logical UE position, which must be known to the eNodeB, rather than the physical location. For example, if UE is physically located in Sector 1, but the strongest received pilot signal is from the beam projected toward Sector 2 because of environmental effects, the UE should be assigned to the beam projecting toward Sector 2, which is its logical position because the UE can experience a superior channel. Therefore, the error between the measured UE position and the exact physical position of UE is not important because eNodeB requires its logical position.

Finally, the solution is summarized as follows:

Step 1: Design an appropriate power disparity of the sub-band for the corresponding sectors.

Step 2: The UE reports the CQI based on the channel condition.

Step 3: The eNodeB determines the position according to the CQI report.

IV. SIMULATION PARAMETERS AND RESULTS

This section discusses the simulations for SINR and the throughput performance of the proposed framework. In the following simulations, the comparisons among the proposed 3 × 3 cell, 3 × 2 cell [1], and 3 × 1 cell [5] are shown.

A. Simulation Parameters

Simulations are performed by modeling antennas in three dimensions. In the proposed 3 × 3 cell, a 16 × 5 uniform planar array (UPA) is used to construct the desired beam pattern, in which both vertical and horizontal antenna spacing are half the wavelength. The parameters used for 3 × 1 and 3 × 2 cells are adopted from [5] and [1], respectively. The detailed simulation parameters are listed in Table I.

B. Simulation Results

The simulated cell throughput results for the 3 × 1, 3 × 2, and proposed 3 × 3 cells are shown in Fig. 4. The overall throughput of the 3 × 3 cell is the best highest among the three cells because of the increased spectral efficiency through frequency reuse. Similar results can also be found in Fig. 5, which shows that the 3 × 3 cell has a 101.6% and a 221.9% improvement on both the average and the worst 5% cell throughput compared with the 3 × 1 cell. Compared with the 3 × 2 cell, the 3 × 3 cell shows a 21.9% and a 39.9% improvement on the average and the worst 5% cell throughput, respectively.

In a 3 × 3 cell, the available resource is three times that of the 3 × 1 cell and one and half times that of the 3 × 2 cell. Conversely, the interference in the 3 × 3 cell is three times that of the 3 × 1 cell and one and half times that of the 3 × 2 cell if the same antenna is used in the three cells. However,

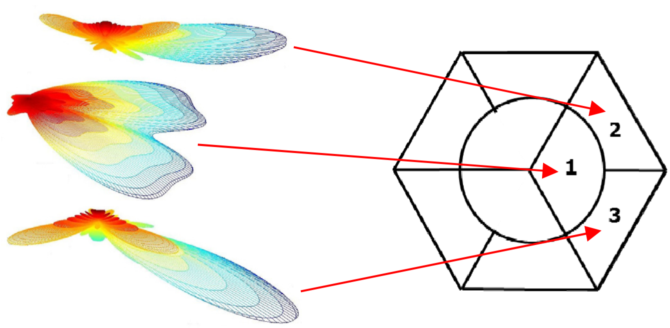

Fig. 2 Beam patterns for sector 1, 2, and 3 of the proposed 3×3 cell

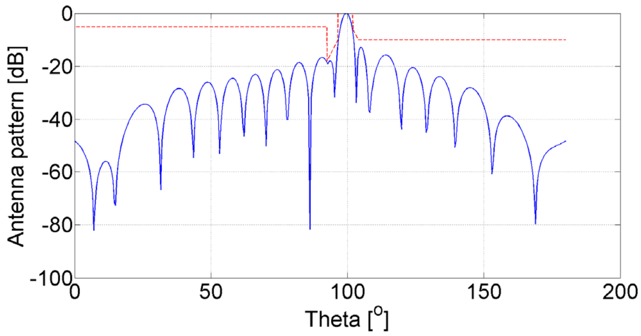

Fig. 3 Vertical beam pattern for sector 3.

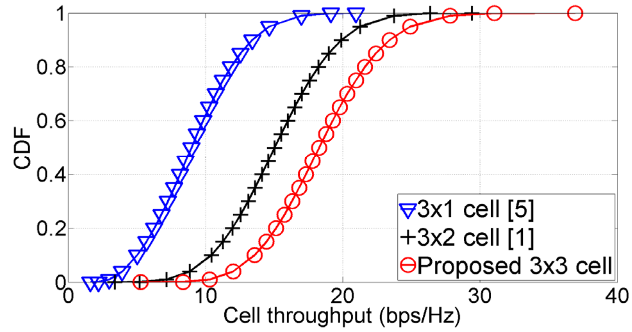

Fig. 4 CDF of cell throughput for 3 × 1, 3 × 2, and 3 × 3 cells, respectively.

TABLE I
SIMULATION PARAMETERS

Parameter	**3GPP case 1**		
	3×1 cell	**3×2 cell**	**3×3 cell**
Network layout	19 eNodeBs		
System frequency	2000 MHz		
System bandwidth	10 MHz		
Frequency reuse factor	1		
Inter-site distance	500 m		
BTS height	32 m		
UE height	1.5 m		
Shadowing STD	8 dB		
Propagation loss model	$L = 128.1+37.6\log_{10}(R)$, R in kilometers		
TX power (per site)	46 dBm		
Antenna techniques	SISO	SISO	MISO
Horizontal HPBW	ϕ_{3dB}=65°	ϕ_{3dB}=65°	ϕ_{3dB}=70°
Vertical HPBW	θ_{3dB}=6°	θ_{3dB}=4.4°	θ_{3dB}=10°
TX antenna gain	Calculated based on antenna characteristics		
Thermal noise per Hz	−174.0 dBm		
Traffic distribution	Uniform		
Traffic model	Full buffer		
Scheduling	Round-Robin		

using an appropriate beam pattern design, the interference in the 3 × 3 cell can be greatly alleviated. However, the cell throughput of the 3 × 3 cell is still larger than that of the 3 × 2 and the 3 × 1 cells because of efficient resource reuse.

The evaluated traffic load of the three cells is listed in TABLE II. Which shows that the 3 × 3 cell has a more balanced traffic load compared with the 3 × 2 cell. Because the 3 × 2 cell uses a mechanical beam tilt instead of an electrical beam pattern design, the geometry of the beam pattern is fixed; however, the geometry of the beam pattern does not match the geometry of the sector. To maximize the overall throughput, the cell is partitioned into six sectors with unequal size; however, in the 3 × 3 cell, the beam pattern is designed to fit the geometry of each pre-determined equal-sized sector. As a result, the traffic load of the 3 × 3 cell is more balanced than the 3 × 2 cell.

TABLE II
TRAFFIC LOAD FOR DIFFERENT CELL SECTORIZATION SCHEMES, WHERE THE NUMBER IS ORDERED IN [1, 2, 3] FOR THE 3 × 1 CELL, [1, 2, 3, 4, 5, 6] FOR THE 3 × 2 CELL, AND [1, 2, 3, 4, 5, 6, 7, 8, 9] FOR THE 3 × 3 CELL, RESPECTIVELY.

	Traffic load for each sector (%)								
3×1 cell	36			32			32		
3×2 cell	5		32	5		27	5		26
3×3 cell	11	11	11	10	11	9	12	11	14

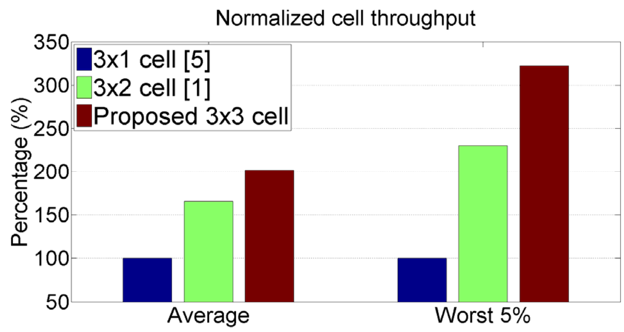

Fig. 5 Cell average and worst 5% throughput for 3 × 1, 3 × 2, and 3 × 3 cells, respectively.

V. CONCLUSIONS

In this paper, a framework of cell sectorization to increase the throughput including a 3D beam pattern design and a sectorization strategy is proposed for a massive MIMO. The strategies used to partition the cell into several sectors have accounted for the traffic load. The beam pattern design based on convex optimization can provide a beam corresponding to the sectorization strategy. Moreover, problems that arise from further cell sectorization were addressed. The simulation results show that the proposed method can provide a fair SINR result and, thus, the spectral efficiency can be increased.

REFERENCES

[1] O. N. C. Yilmaz, S. Hämäläinen, and J. Hämäläinen, "System level analysis of vertical sectorization for 3GPP LTE," in *Proc. IEEE Conf. ISWCS*, Sep. 2009, pp. 453-457.

[2] M. Caretti, M. Crozzoli, G. M. Dell'Aera, and A. Orlando, "Cell splitting based on active antennas: performance assessment for LTE system," in *Proc. IEEE Conf. WAMICOM*, Apr. 2012, pp. 1-5.

[3] H. Huang, O. Alrabadi, J. Daly, D. Samardzija, C. Tran, and R. Valenzuela, "Increasing throughput in cellular networks with higher-order sectorization," in *Proc. Asilomar Conf. Signal, Systems, and Computers*, Nov. 2010, pp. 630-635.

[4] S. E. Nai, W. Ser, Z. L. Yu, and H. Chen, "Beampattern synthesis for linear and planar arrays with antenna selection by convex optimization," *IEEE Trans. Antennas Propag.*, vol. 58, no. 12, pp. 3923-3930, Dec. 2010.

[5] 3GPP TR 36.814 V9.0.0, Evolved Universal Terrestrial Radio Access (E-UTRA); Further advancements for E-UTRA Physical layer aspects.

[6] S. Boyd and L. Vanderberghe, *Convex Optimization*, Cambridge University Press, 2004.
[7] 3GPP TR 36.213 V11.2.0, Evolved Universal Terrestrial Radio Access (E-UTRA); Physical layer procedures.